Applied Thermal Engineering 218 (2023) 119309

Contents lists available at ScienceDirect

Applied Thermal Engineering

journal homepage: www.elsevier.com/locate/apthermeng

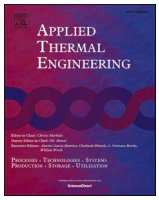

Proposal of a thermocline molten salt storage tank for district heating and cooling

A. Abánades [a,*], J. Rodríguez-Martín [a], J.J. Roncal [a], A. Caraballo [b,1], F. Galindo [b]

[a] Universidad Politécnica de Madrid; ETSII, c/José Gutiérrez Abascal, 2, 28006 Madrid, Spain
[b] FERTIBERIA, Paseo de la Castellana, 259D, 28046 Madrid, Spain

ARTICLE INFO

Keywords:
Low melting temperature molten salts
District heating and cooling
Thermocline tank

ABSTRACT

Thermal Energy storage is one of the critical components in district heating and cooling (DHC) facilities when based on intermittent energy sources (as solar). Currently, DHC energy storage is based on water tanks. Nevertheless, water storage cannot be used with medium temperature processes as double effect absorption chillers or other services requiring temperatures well above 100 °C. Current thermal storage at higher temperature may be based on a variety of technologies. Among then, molten nitrate salts are widely used for heat storage in concentrated solar plants (CSP), limited by the melting temperature of available commercial solar salts and their solidification risk. Such commercially available salts are not applicable to district heating and cooling as they are solid in the expected operational temperature range. Other storage media may be solid materials, either by the use of packed-bed materials, concrete or phase change materials.

In this paper, an innovative molten salt mixture with a melting temperature below 150 °C is used. The availability of a storage medium in a temperature range from 150 up to 250 °C might increase the solar share in DHC installations, integrating concentrated solar technologies. Such storage allows to apply solar technologies to supply heat to services for DHC that now can be only provided by boilers. In this communication, a molten salt storage tank operating in thermocline mode will be proposed in the framework of the WEDISTRICT project [1]. The project seeks to deliver the highest possible share of renewable sources for the energy needs of a district demand, maximizing performance by the application of advanced absorption chillers, that requires temperature feeds well above 100 °C.

1. Introduction/background

Household energy demand constitutes a significant part of the energy consumption in the European Union [2]. According to Eurostat, 28 % of the total energy use in the EU-27 is consumed in the household sector with more that 48 % based on fossil fuels (coal, natural gas, liquified petroleum gases or diesel) [3]. Energy decarbonization in Europe requires the implementation of low-carbon technologies in district heating and cooling facilities [4]. From this perspective, the WEDISTRICT project seeks to deliver the highest possible share of decarbonized energy for a district heating and cooling demand. A variety of thermal renewable technologies are developed and tested up to TRL7. Technology integration in the project includes generation (biomass, geothermal, solar,.) energy harvesting/recovery technologies, and innovative thermal cooling systems [5]. Energy storage plays a pivotal role in such integration. The WEDISTRICT project will be implemented in three demo-sites corresponding to different types of district demand and climate regions within Europe: a) Lulea in Sweden will install a fuel cell in hybridation with waste heat from a data centre cooling; b) a faculty building of the Politehnica University in Bucharest will be covered by a combination of solar PV and geothermia; and c) a heating and cooling network with a low-emission biomass boiler, several types of solar technologies (Fresnel, parabolic troughs, and a low concentration flat plate collector), and different technologies to provide the heating and cooling demand, as absorption chillers in Alcalá de Henares (Spain).

Efficient thermal cooling technologies based on advanced absorption systems, and optionally some other services (local industrial processes as vapour cleaning or desinfection), into heating and cooling networks, requires to deliver heat at temperatures well above 100 °C. Therefore, only manageable energy sources as fossil (natural gas, or coal), and

* Corresponding author.
E-mail address: abanades@etsii.upm.es (A. Abánades).
[1] Current address: Universidad Politécnica de Madrid, c/José Gutiérrez Abascal, 2, 28006 Madrid, Spain.

https://doi.org/10.1016/j.applthermaleng.2022.119309
Received 12 January 2022; Received in revised form 15 July 2022; Accepted 8 September 2022
Available online 14 September 2022

biomass are implemented up to day to fulfil the energy needs, for instance, of double effect absorption chillers. Double effect absorption chillers have the same basic components of single-effect, but coupling two of those absorption cycles with additional generator, heat exchanger and pump. The heat rejected by one of the cycles feeds the other one. A good performance with those type of absorption chillers (COP > 1.2) configuration requires upper temperatures higher than 100 °C. Such equipment is generally driven by natural gas.

Thermal energy storage for concentrated solar power is commercially available by molten salt accumulation in two isothermal tanks [6], and tested by thermocline tanks [7]. The operation of concentrated solar power plants (CSP) is intended at higher temperature as technically feasible to provide the highest achievable plant efficiency. Nitrate salts [8] are the commercial standard as Heat Transfer Fluid (HTF) for this purpose, with operational ranges roughly between 250 and 600 °C due to its melting point (above 200 °C) and their degradation rate at high temperatures. Carbonates [9] have been proposed as well to increase the upper temperature operation. Thermocline tanks has been proposed as an alternative for two isothermal tanks for their lower potential cost. Such thermocline tanks has been tested, either with several heat transfer carriers as air [10], oil [11], and molten salts [12] with very well established numerical model validation. Unfortunately, none of those alternatives already developed or under development are suitable for district heating and cooling applications in the medium temperature range (130–300 °C). Another alternative is the utilization of phase-change materials (PCM) [13,14], but their application is not compatible with the usual temperature difference on the service and return energy flows of a district heating. The choice of the phase-change material fixes the temperatures for charge/discharge in a narrow range, limiting the adaptation of the storage to the temperatures of the demand, and affecting its control strategy.

Up to know, molten salts are not currently applied to DHC due to the high melting temperature for most of the commercially available molten salts. Decomposition and degradation of the salts are an issue in the long term, provoking high operation costs and maintenance problems. In any case, degradation is very low at the temperatures intended to be set in district heating. Another aspect to consider is the corrosion induced by molten salts in current tank and loop structural materials as steel. Corrosion at the temperatures as expected in DHC facilities is reported to be very low even in common carbon steels, what will be discussed in the next section.

As a result of this analysis, the application of molten salt storage for district heating and cooling (DHC) installation requires the development of new salt mixtures that could overcome the solidification risk of state-of-the-art solar salts. The application window for molten salts in DHC is open if their solidification could be well below 150 °C. This is the main challenge of the application of molten salt storage tanks to the residential sector, and one of the main innovations regarding storage technology into the WEDISTRICT project [1], where a variety of new technologies will be tested. A molten salt tank, operating between 150 and 235 °C, described in next sections is proposed for the Alcalá site mentioned below.

The description of the characteristics of nitrate-based molten salt mixtures, able to operate below 150 °C is the main content of the next section. A proposal to test such mixtures in relevant operational conditions is the main novelty of this paper. Nitrate salts have not been previously applied for district networks. Temperature requirements in district heating loops are much lower than in solar thermal plants. In particular, corrosion risks are drastically reduced for low melting temperatures.

Further sections will describe a thermocline tank for the verification of the operation of those new salt applied to a DHC network. There has been previous works in the field of modelling [15–17] and experimental analysis of this kind of tanks, either filled with water in domestic application [18] or molten salts at higher temperatures for CSP. Special attention is paid to the analysis of the stratification [19] and temperature position of the thermocline layer. Such previous work shows how there are some key challenges for the implementation of molten salts for temperatures up to 235 °C. Solidification risks is solved partially by the development of the low melting temperature salts described in next section. Thermocline layer stability is controlled by a continuous charge/discharge of the system and the utilization of a filling material providing less thermal diffusion at the thermocline layer. On the other hand, the economic viability of the storage is improved by the addition of cheap materials as packed bed in the tank. Based on that experience, the conceptual design of the tank to be commissioned in WEDISTRICT is presented.

2. Molten salt preparation for district heating and cooling operation range

The composition of ternary salts based on Strontium, Sodium and Potassium nitrates ($Sr(NO_3)_2$, $NaNO_3$, KNO_3) has been screened, searching from combinations and eutectic compositions that could provide a low melting point molten salt mixture. Additionally, quaternary mixtures adding Calcium nitrates ($Ca(NO_3)_2$) and Sodium nitrides ($NaNO_2$) have been tested. A first literature review was done to analyse the commercial suitable candidates in combination with thermodynamic modelling using CALPHAD methodology [20], to evaluate thermal-physical properties for combination of materials and salts [21,22] and their phase diagrams. From the evaluation of a set of combination of nitrate salts, ternary diagrams, as the example shown in Fig. 1 are produced, in this case just for $Sr(NO_3)_2/NaNO_3/KNO_3$ combinations. In the figure is shown the phase diagram of the binary mixture $NaNO_3/KNO_3$ as one of the input data, that combined with the phase diagrams of the rest of components of the salt enables the prediction of thermal-physical properties, as the melting point of eutectic combinations.

As a result of the work carried out with the combination of alkali and alkaline earth nitrates and nitrites, a quaternary salt has been produced for its testing in the WEDISTRICT storage tank in Alcalá, denoted as FERT-1 ($Sr(NO_3)_2/NaNO_3/KNO_3/LiNO_3$ (5/17/49/29 % wt/wt)), adding $LiNO_3$, as suggested as well from previous publication [23] and patents [24]. The thermal-physical properties of such salt have been estimated by the CALPHAD methodology by the composition of the properties of the salt components and checked by DTA and XRD analysis in the laboratory. Density, viscosity, specific heat capacity, and thermal conductivity has been measured and compared with the Solar Salt (state-of-the-art thermal energy storage (TES) material [25], $NaNO_3/KNO_3$ 60/40 % wt/wt [26]) for the liquid phase, as shown in Fig. 2. Main differences are observed in heat capacity with around 10 % improvement depending on temperature, being similar the rest of thermal-physical properties.

Corrosion behaviour of the TES material was one of the main concerns for the design of the system. Conventional stainless steels have been tested 2000 h with FERT-1 salt at 425 °C. Rectangular, tube, weld and under stress probes were tested in order to determine general, intergranular, weld and under stress corrosion. The results show corrosion rates below 0.1 mm/y for every stainless steel, including AISI 430.

As a reference for the material selection for the tank, the work of Fernández et al. [27] shows a rigorous corrosion analysis for nitrate-based salts. Their corrosion results for AISI 304 as reference austenitic steel, and AISI 430 as ferritic steel (Fig. 3) shows that corrosion drops drastically with temperature, being the expected WEDISTRICT operation well below 390 °C, which would allow the safe utilization of austenitic or ferritic steels. To cross-check that assumption, the corrosion impact of FERT-1 for a set of stainless steels were also performed and evaluated by the immersion during 2000 h at 425 °C of rectangular, tube, weld and under stress probes to determine general, intergranular, weld and under stress corrosion. SEM analysis, weight loss, and EDX studies were carried out to evaluate corrosion with AISI 304, 347, 321,

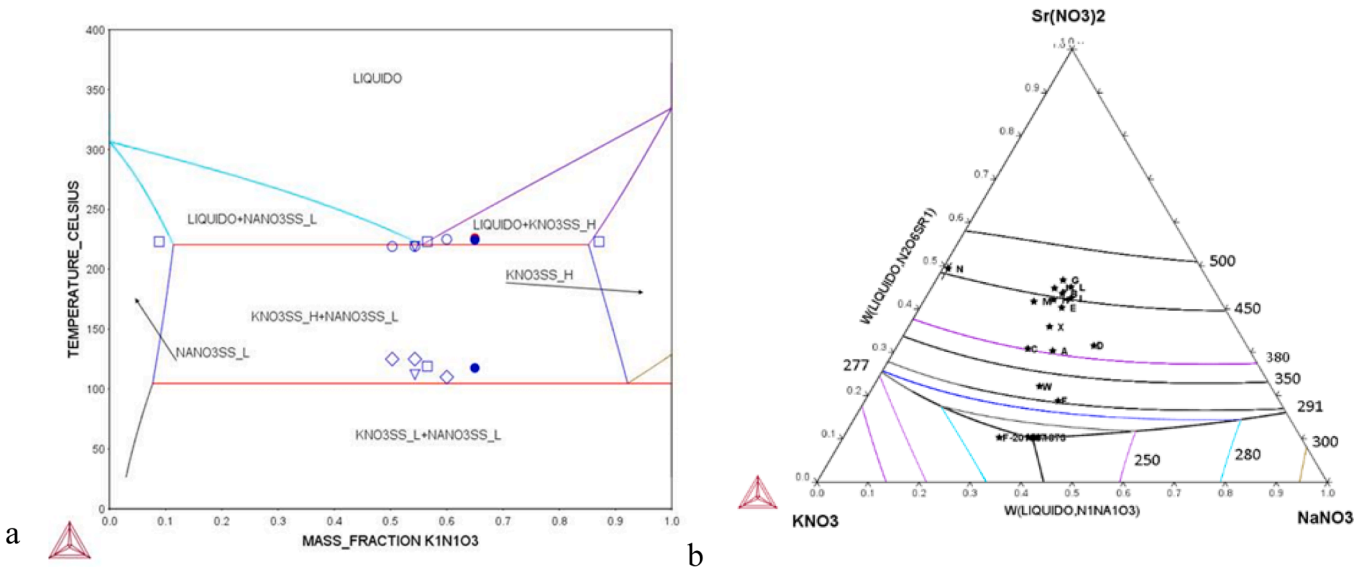

Fig. 1. Example of ternary diagram modelled for Sr/K/Na nitrates (b) from binary phase diagrams as (a).

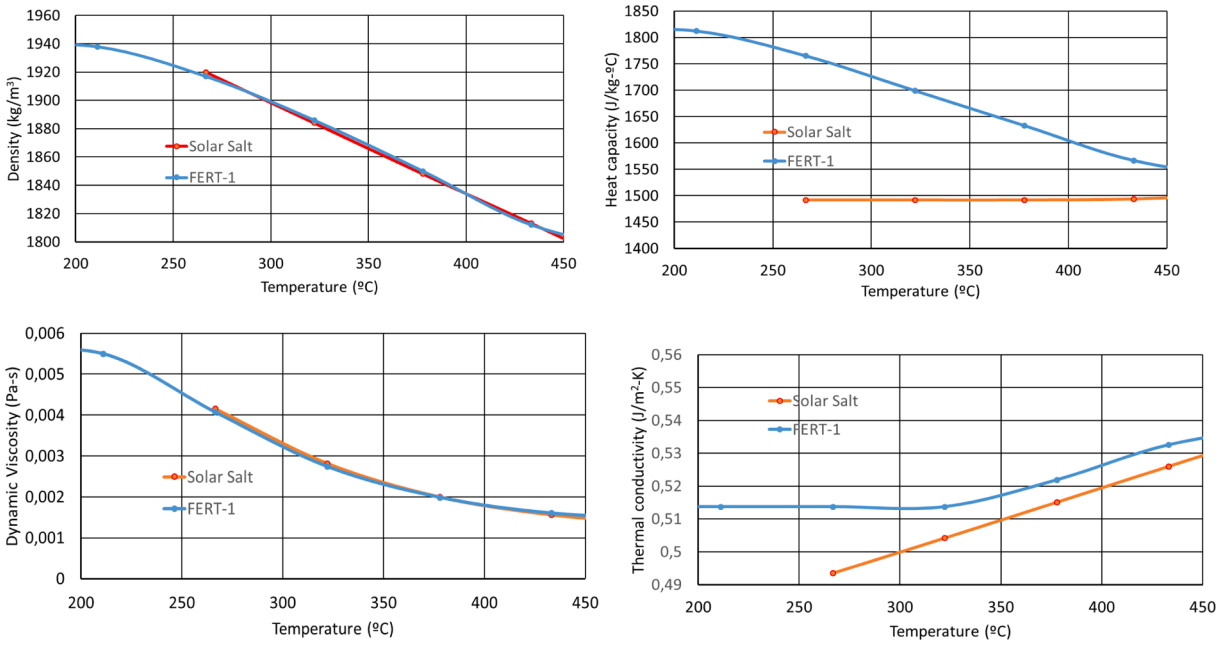

Fig. 2. Thermal-physical properties of the FERT-1 mixture and the Solar Salt.

316, 318, 316Ti and 430 stainless steels. Results shows corrosion rates less than 100 μm/year in all cases at 425 °C (Fig. 4) for the FERT-1 molten salt.

The low temperature operation gives the possibility of using carbon steels as 516 Gr 70, that are affected by a high corrosion rate at T > 400 °C, but acceptable below 300 °C, allowing lower costs, as well as better delivery and manufacturing in more competitive time frames. To increase structural safety respect to corrosion it is proposed a corrosion allowance of 3.2 mm as over-thickness of the wall steels for the nominal design.

Another important issue is the stability of the eutectic mixture. Two kinds of reactions can occur at high temperatures for nitrate mixtures. In the case of alkaline nitrates, it decomposes into the nitrite. Nitrites are highly soluble in nitrates and their presence leads to a decrease in the freezing point of the mixture. Nitrites can decompose into alkaline oxides, nitrogen and nitrates again. This mixture can rapidly react to produce alkaline hydroxides (very corrosive) and carbonates. These species present a limited solubility in molten nitrates, so they can precipitate leading to problems with valves and pipelines. Such problem is critical at high temperature operation [21,28,29]. In the case of the WEDISTRICT project, temperatures are expected well below 250 °C, being under the threshold to activate this second transformation for alkaline nitrates. The decomposition of salt nitrates into nitrogen and nitrogen oxide is a risk that has been tested for the quaternary salt mixture. DTG (Differential thermogravimetry) and DTA (Difference thermal analysis) gives the diference in mass in the sample respect to the reference level and it is a measure of the degradation of the salt. A tertiaty eutectic (ET) and quaternary eutectic (EC) has been tested between 30 and 1000 °C (Fig. 5). As a conclusion, for the quaternary eutectic salt FERT-1, a temperature range of 110–500 °C is safe regarding stability criteria.

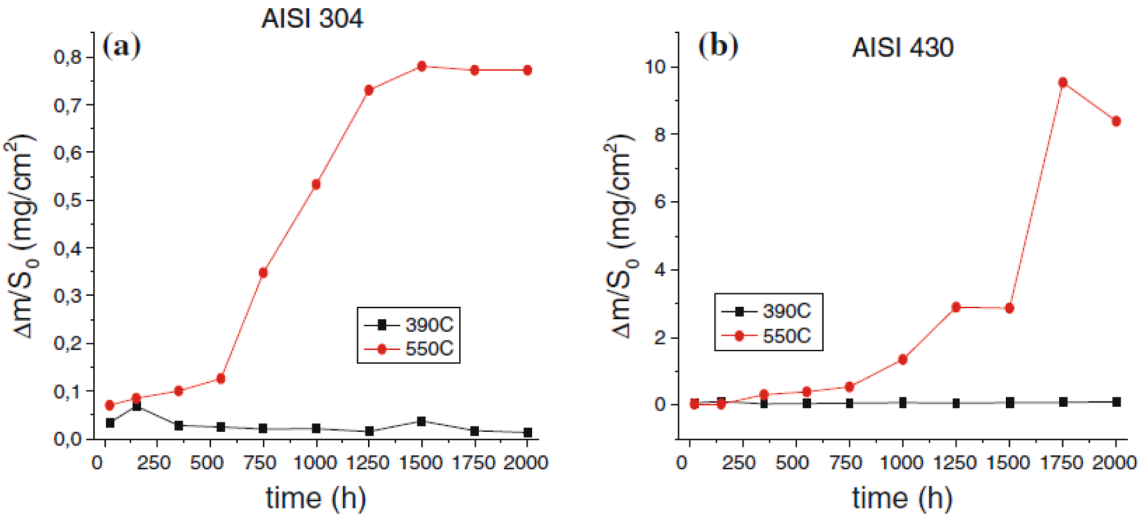

Fig. 3. Corrosion test on AISI 304 and AISI 430 steel extracted from [27].

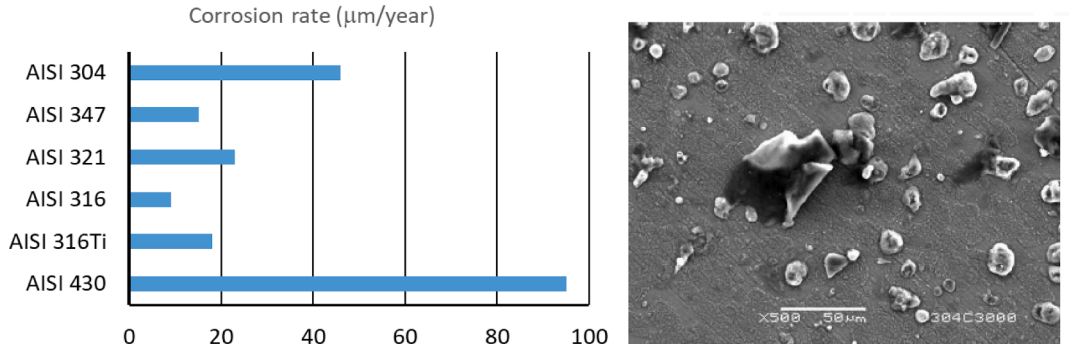

Fig. 4. Corrosion rates (µm/year) of FERT-1 in selected steels and SEM images of AISI 304 after 2000 h at 425 °C.

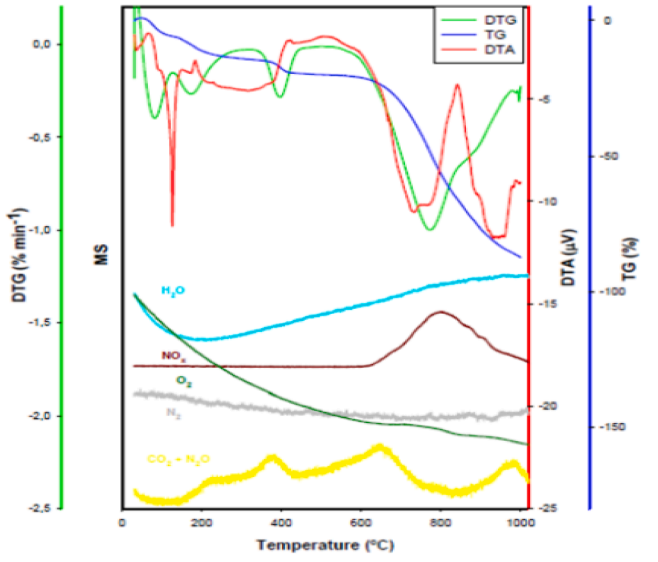

Fig. 5. DTG and DTA analysis for eutectic ternary (ET) and quaternary (EC) salts.

3. Molten salt tank proposal for WEDISTRICT

The described quaternary molten salt denoted as FERT-1 is being proposed in combination with a packed bed of quartzite rocks for the storage of heat produced by concentrated solar technologies developed in the WEDISTRICT project. Solar technologies will be based on the utilization of a Fresnel field and parabolic trough collectors operating between 250 and 210 °C, as defined in the project WEDISTRICT [1] The heat from the solar collectors will be transferred by a heat exchanger to the FERT-1 molten salt, that will operate the tank between 235 and 150 °C. At tank charge, the connecting heat exchanger will increase the enthalpy of the molten salt circulating between the auxiliary cold tank and the cold tank driven by the pump embedded in the cold tank. At discharge, the pump submerged in the hot auxiliary tank will send hot molten salt to reduce its enthalpy trough the intermediate heat exchanger towards the cold auxiliary tank, that will buffer the salt before flowing via the storage tank bottom. A sketch of the integration of the storage tank is shown in Fig. 6.

The storage tank that is proposed has as most important parameter for its design, the storage capacity that will be needed for the the Alcalá demo-site in view of the demand and the solar generation. From the storage capacity point of view, the rest of the conceptual and physical design of the tank will be elaborated based on 1-D model, as well as dynamic model to estimate the response of the tank. From the available information, a proposed design for the storage tank will be delivered for its detailed engineering and commissioning.

As the WEDISTRICT facility at Alcalá will hold a biomass boiler as back-up, the storage capacity of the tank has been evaluated from the analysis of the annual production of the solar field of the Alcalá site in WEDISTRICT. Winter demand is mainly for heating. In summer, cooling is provided by thermal system, as absorption chillers. The size of the molten salt storage has been chosen according with the following criteria:

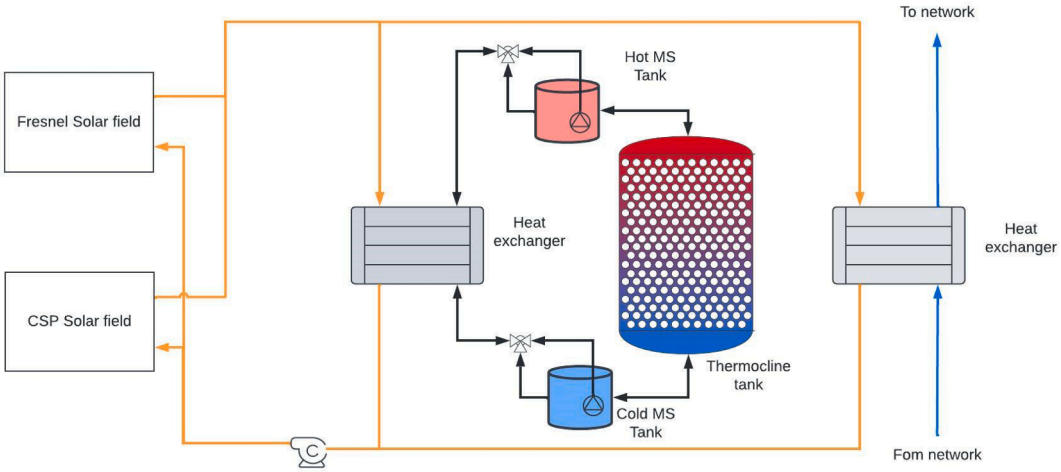

Fig. 6. Integration of molten salt storage into WEDISTRICT.

- The storage is sized for the accumulation of available energy in daily basis, following load cycles when solar irradiation might be available, and discharge during the rest of the time. The maximum expected daily energy production is 4.5 MWh/day in summer, as shown in Fig. 7. The total nominal power of the concentrated collectors is of 411.35 kW.
- Scale for demonstration purposes: The storage capacity in molten salts should be done at a scale suitable to demonstrate the utilization and performance of the technology in a real district heating and cooling environment. Storage capacities of the order of MWh should be enough to achieve operational experience in production environments.

Fig. 7 shows the accumulative distribution of daily solar production along the year. This information shows that there are >215 days in the year producing less than 2 MWh. Following these criteria, the storage capacity of the molten salt tank has been set to 2 MWh, to operate with solar production availability, keeping the storage volume into the budget restrictions of the WEDISTRICT project, that, for instance, constraints the molten salt inventory to 30 m^3, as molten salt cost is estimated to be of the order of 1 €/kg and complying with the practical increase in TRL, testing the performance of a storage system into a relevant practical environment. Carbon steel as tank material contributes to reduce costs, as well as the implementation of a packed bed formed by cheaper material, that reduces the molten salt inventory and improve the stability of the thermocline layer.

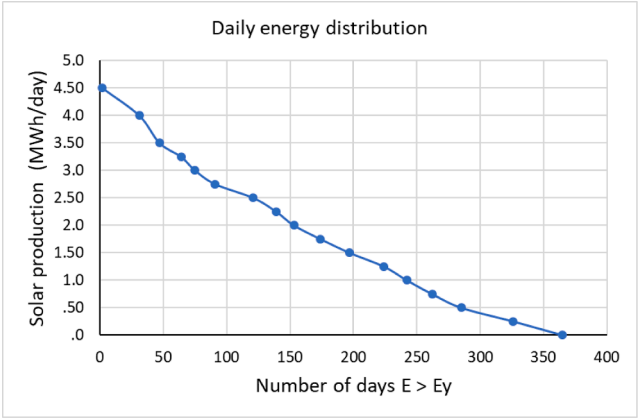

Fig. 7. Accumulative distribution of daily solar production in Alcalá site.

4. Steady-state model for nominal design

The design of a thermocline tank filled with molten salt is based on a cylindrical steel tank with distributors at the inlet and outlet of the salt, and a vast central region filled with a packed bed. The packed bed has a very important impact on the stability of the thermal profile of the tank and its capacity, as described by the other authors [16]. An Engineering Equation Solver model has been developed to evaluate the basic parameters of the thermocline tank vessel, including the mass and energy flow balances.

The tank is modelled by an effective storage volume, where the thermocline layer should be located at any time, some space for fluid buffering, and two auxiliary tanks that absorbs fluctuation of the molten salt flow at charge/discharge. In those auxiliary tanks, the molten salt pumps are immersed. The main tank is filled with quartzite rocks [30], with a porosity or void fraction (ε) of 0.25 [31]. The thermal capacity of the effective storage volume is estimated by the aggregation of the molten salt and rock-bed capacities as:

$$\overline{\rho \bullet C_{p_{eff}}} = \left(\rho \bullet C_p\right)_{salt} \bullet \varepsilon + \left(\rho \bullet C_p\right)_{rock} \bullet (1-\varepsilon) \quad (1)$$

Being ε, the porosity of the rock, the total energy accumulated in the effective storage volume ($V_{eff,st}$) is estimated from the density of the combination of molten salt and quartzite as:

$$E = \overline{\rho \bullet C_{p_{eff}}} \bullet V_{eff,\,st} \bullet \Delta T \quad (2)$$

The total volume of the tank is evaluated as the effective storage tank plus the volume that is assigned for upper and lower buffering, including the vessel head. From the rest of the storage requirement, as the exchange power, the mass flow rate of the molten salt to enter the tank is estimated.

From the definition of the tank, there are some features of great interest for the diagnosis of the tank performance. From the exchange power, either for charging or discharging of the storage, the mass balance in the tank is defined by the equation:

$$Q = \dot{m}_{salt} \bullet C_{p,salt} \bullet (T_{max} - T_{min}) \quad (3)$$

The equivalent storage time, meaning the time to completely discharge the full storage capacity providing the nominal exchange power, is:

$$C_t = \frac{E}{Q}$$

Producing a nominal inlet mass-flow rate of molten salt during the charge of the tank:

$$\dot{m}_{salt}[kg/s] = \frac{Q\ [W]}{C_{p,\ salt}\left[\frac{J}{kg^{\circ}C}\right]\cdot(T_{max} - T_{min})[^{\circ}C]} \tag{4}$$

The mass-flow should flow through the packed bed. The average flow velocity in the bed is one of the criteria for the stability of the thermocline layer. The average velocity depends on the porosity of the packed bed, that gives an estimation of the mean constraint of the molten salt flowing cross section. The average velocity is then:

$$u[m/s] = \frac{\dot{m}_{salt}[kg/s]}{\varepsilon \bullet A_T}$$

The dimensions of the tank, and the characteristics of the porous filling will serve to check the stability criteria of the thermocline layer, and the pressure loses due to the molten salt displacement inside the tank. In particular, the stability criteria is established [19] by the evaluation of a critical velocity from the properties of the hot salt (1) and the cold salt (2).

$$u_c = gK\frac{(\rho_1 - \rho_2)}{(\mu_1 - \mu_2)} \tag{5}$$

With g as the gravity, the density and viscosity differences and the conductivity K. For the FERT-1 salt, both the viscosity and the density are decreasing versus the temperature, being u_c positive. If the velocity of the salt into the tank is lower that the terminal velocity, the thermocline layer is stable during charge and discharge. For the tank operation, with a power exchange of 411 kW, it has been checked that velocities in the smaller tanks are well below 7.65 mm/s, that is the critical velocity.

The pressure losses in the tank are evaluated with the Ergun equation, applicable to porous media.

$$\frac{\Delta P}{H_{sto}} = \frac{150 \bullet \mu}{d_p^2} \bullet \frac{(1-\varepsilon)^2}{\epsilon^3} \bullet u_f + \frac{1,75 \bullet \rho}{d_p} \bullet \frac{(1-\varepsilon)}{\epsilon^3} \bullet u^2 \tag{6}$$

The particle diameter of the rocks in the bed is a parameter that depends on the size of the rock stones and its physical meaning is similar to a dimension characteristic length. The pressure losses may change slightly with the variation of the average thermal-physical properties of the salt in the porous media versus temperature.

The steady-state model has been implemented in Engineering Equation Solver (EES) [32] to evaluate the nominal design parameters. Fig. 9 shows a screenshot of the diagram window of the EES model. The nominal design of the storage tank is summarized in Table 1.

A critical aspect that determines the performance of a single thermocline tank is the thermocline thickness and its stability. There are some criteria to be fulfilled for the evaluation of a correct performance of a thermocline tank [19]. During the operation of charging a thermocline tank, the hot molten salt is charged in from the top inlet of the tank. When the hot molten salt displaces the cold one in the porous medium of the tank, viscous fingering is likely to occur. On the other hand, however, gravity is a stabilizing factor that tends to keep the interface horizontal due to the density difference of the two fluids. Therefore, from the consideration of these two factors: viscosity and density, the process of the hot molten salt displacing the cold one downwards may be stable or unstable depending on which of the two factors is predominant.

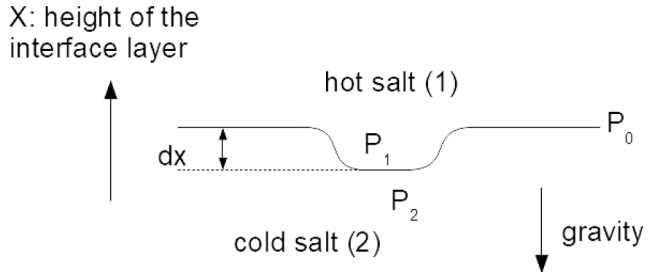

Fig. 8. Interface between hot and cold molten salt at the thermocline layer.

The gravity and the density difference by thermal expansion keeps the hot molten salt in the upper part, in opposition to the viscosity differences that drives the fingering of the hot molten salt into the cold one. The effect of the density should be higher than viscosity, being the pressure at the cold side higher than the hot side. Following the scheme of the Fig. 8, the stability criterion to be fulfilled is:

$$P_1 - P_2 > 0 \tag{7}$$

The pressure in the hot side is obtained from the reference pressure level (P_0) and the effect of the density, and the viscosity pressure losses (u is the displacement velocity of the fluid at charging):

$$P_2 = P_0 + \rho_2 g\delta x - \frac{\mu_2 u\delta x}{K} \tag{8}$$

The criteria expressed in Eq. 5 is then expressed as:

$$(\rho_1 - \rho_2)g\delta x - \frac{(\mu_1 - \mu_2)u\delta x}{K} > 0 \tag{9}$$

Defining a critical velocity for the evolution of the thermocline level as expressed in equation 5.

Therefore, the stability criterion is positive when the velocity of the molten salt in the tank is lower than the critical velocity. Such velocity is evaluated in the steady-state model to check that design parameters and charge/discharge nominal values comply with the stability criteria of the thermocline layer.

5. Dynamic model

A numerical analysis implemented in MATLAB [33] solves a 1-D model in accordance with the basic scheme depicted in Fig. 10. The model describes an inlet mass flowrate, either hot at the top or cold at the bottom, and an outlet molten salt flow rate. The tank is assumed to be a vertical cylinder filled by a porous media. The cylinder is divided in N segments. The molten salts flow through those segments that are considered as nodes for the resolution of the balance equations. Each cylindrical node is defined by the tank diameter (D) and node height (Δx), and characterized by a homogenization of the thermal-physical properties and its temperature.

The model solves the energy balance of each node according to classical heat transfer [34]. Considering that each node is composed of a solid material and the molten fluid, the energy balance at each node is defined by the following equations:

In the molten fluid:

$$\varepsilon(\rho c_p)_f\frac{\partial T_f}{\partial t} + \varepsilon u(\rho c_p)_f\frac{\partial T_f}{\partial x} = k_{eff}\frac{\partial^2 T_f}{\partial x^2} + h_{sf}A_{s,f}(T_s - T_f) + U_w a_w(T_{env} - T_f) \tag{9}$$

In the solid material:

$$(1-\varepsilon)\rho_s c_{p,s}\frac{\partial T_s}{\partial t} = h_{sf}A_{s,f}(T_f - T_s) \tag{10}$$

what includes:

- The variation of internal energy due to the temperature change with time (δT/δt [°C/s]), that depends on the thermal capacity of the fluid (ρc_p), being ε the porosity of the packed bed material, what is occupied by the flow material.
- The energy variation due to the mass flow of molten salt, that depends on the flow velocity (u [m/s]) and the temperature gradient in the tank (δT/δx [°C/m]):
- The heat diffusion trough each cell, that depends directly on the effective thermal conductivity of the material (k_{eff}) based on the Gonzo equation [35], that follows the following formulation based

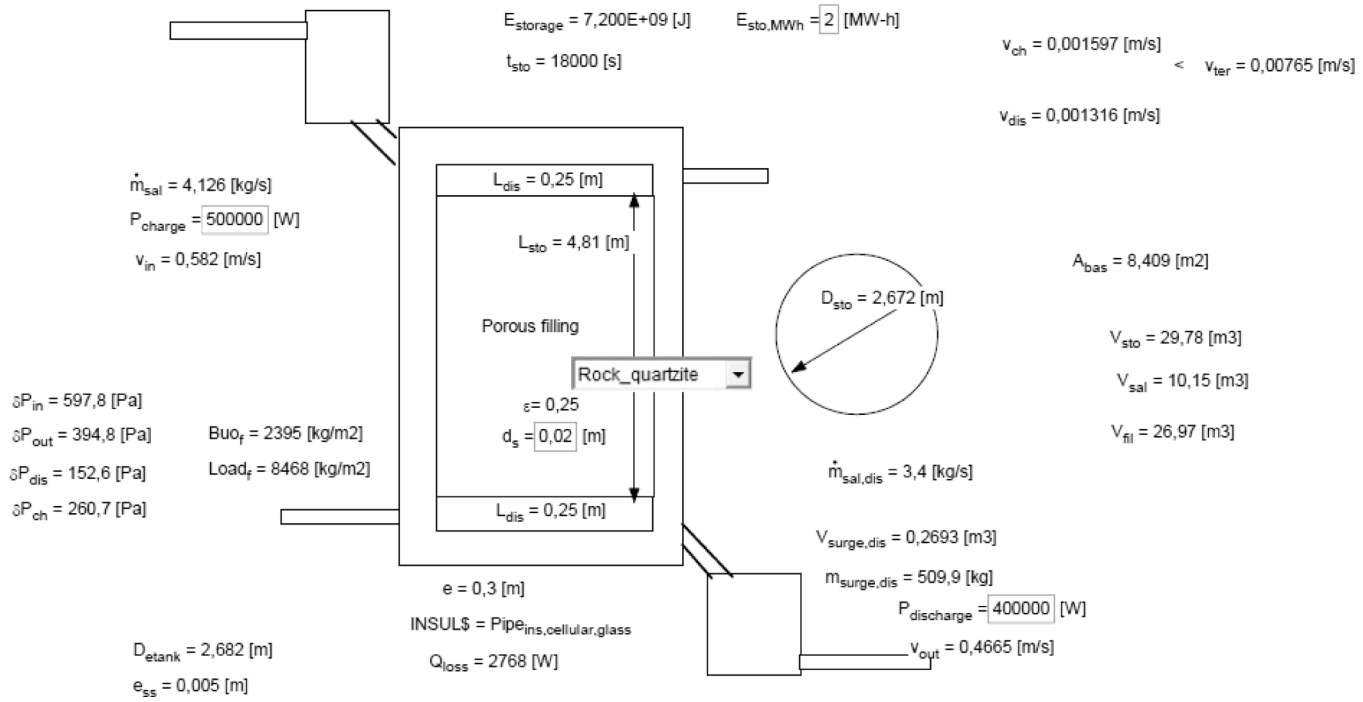

Fig. 9. Diagram window developed into EES software package.

Table 1
Nominal specification for the molten salt storage tank.

Specification	Value	Unit
Storage capacity	2	MWh
Exchange power	411.3	kW
Max. temperature	235	°C
Min. Temperature	150	°C
Rock type	quartzite	
Tank volume	33.58	m^3
Effective volume	30.53	m^3
Tank inner diameter (D_{sto})	2.785	m
Tank height (H)	5.513	M
Active height (H_{sto})	5.013	M
Bed porosity (ε)	0.25	–
Salt velocity in tank for stability evaluation	1.3 (charge); 1.5 (disch.)	mm/s
Molten salt in tank	10.68	m^3
Rock volume	22.9	m^3

on the porosity of the solid material (ε) and the solid and fluid conductivity (k_s and k_f):

$$k_{eff} = k_f \frac{1 + 2 \bullet \beta\phi + 2 \bullet (\beta^3 - 0.1\beta)\phi^2 + 0.05\phi^3 exp(4.5\beta)}{1 - \beta\phi} \tag{11}$$

being

$$\phi = 1 - \varepsilon \tag{12a}$$

$$\beta = \frac{k_s - k_f}{k_s + 2 \bullet k_f} \tag{12b}$$

- The heat transfer between the fluid and the solid material by convection (coupling energy balance equations in solid and fluid phases), what is calculated as function of the heat exchange surface per unit volume ($A_{s,f}$ [1/m]), a convection coefficient ($h_{s,f}$ [W/m2-°C]) and the temperature differences between both phases. The exchange

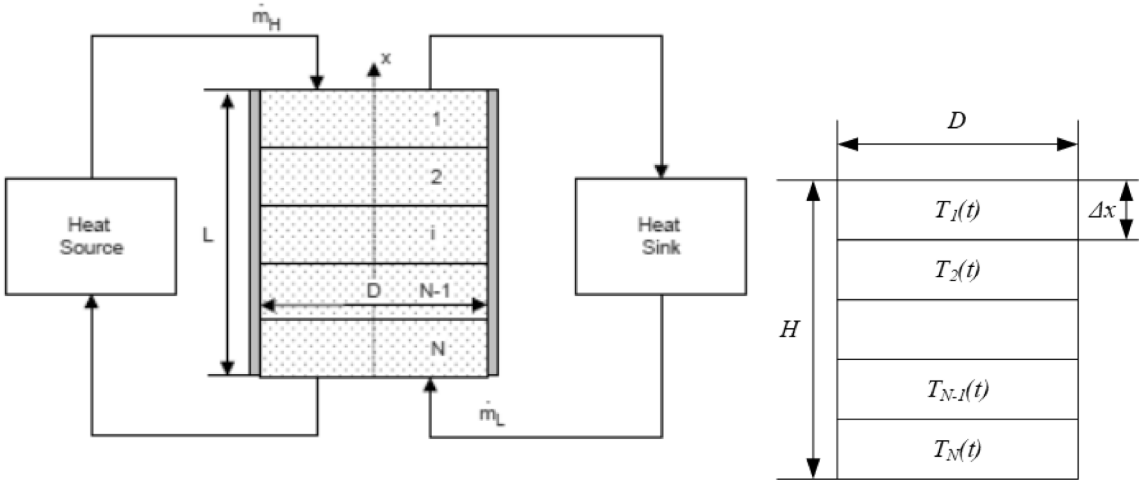

Fig. 10. Scheme of the dynamic model of the tank.

area is estimated assuming that the packed bed is formed by spherical particles as proposed by Raccanello [16]. The convection heat transfer coefficient around the packed bed particles is estimated by the Nusselt correlation [15]. Reynolds and Prandtl numbers are defined from the flow velocity, the particle diameter, the porosity:

$$Nu_{sf} = \left(2 + 1.1 \bullet Re_p^{0.6} \bullet Pr^{1/3}\right);\ h_{sf} = \frac{k_f}{d_s}\left(2 + 1.1 \bullet Re_p^{0.6} \bullet Pr^{1/3}\right) \quad (13)$$

The model has been qualified with available data in literature of a water thermocline tank [17] and the proposal for thermal storage in the SolarOne plant for a storage capacity of 170 MWh, with the Caloria HT-43 thermal oil, into a tank with rock and sand as porous filling material [35]. The results of those qualifications are shown in Fig. 11.

The comparison of our model with available data for a water thermocline tank is done for a 0.4 m-height 1.4 m- diameter cylindrical tank, operating between 25.9 and 50.8 °C and 42 m^3 [17]. Fig. 11a) shows the data published by Bayón et al. and the prediction of the thermocline layer position by our model. The main statistical comparison between our model and the reported data is shown in Table 2. The mean temperature difference between reported and calculated temperatures at the thermocline layer is less than 3 %. A similar analysis has been done for the data of the SolarOne plant. In this case, data has been reported during discharged, at the start (t = 0) and after 4 and 8 h. The SolarOne tank is a 12 m-height, 18.2 m-cylindrical container of Caloria HT thermal oil filled with rocks and sand. In this latter case, the operating temperatures of the oil are 179.2 and 295.2 °C, for a ΔT = 116 °C. Fig. 11b shows the graphical comparison between the data reported and our model. The statistical analysis of the model is shown in Table 2. During discharge, temperature difference between data and simulation are limited to 5.37 °C after a discharged period of 8 h, what means a mean deviation of the order of 5 %.

The application of the dynamic model to the nominal design described in Table 1 in Fig. 12, normalized into the effective volume.

6. Conclusions

Energy storage for district cooling is now performed under the limitation of the liquid phase range of water, restricting cooling to single-stage absorption chillers. The utilization of molten salts enables the increase in temperature. They are commercially used for thermal storage in solar thermal plants, traditionally seeking higher operational temperatures than DHC. Nevertheless, commercially available nitrate salts have a safe liquid range that is not suitable for household and other service applications below 200 °C, mainly due to solidification risks. In the framework of the WEDISTRICT project, new nitrate salt mixtures are under development and testing with the main aim to operate below 150 °C, making feasible the implementation of thermal storage well above 100 °C for district heating and cooling. Based on a new quaternary salt, called FERT-1, composed by a $Sr(NO_3)_2/NaNO_3/KNO_3/LiNO_3$ mixture, a thermocline storage tank is designed and proposed for the commissioning in the Alcalá demo of the WEDISTRICT project. Thermal-physical properties and corrosion test has been performed to check material compatibility and sizing of the tank. In particular, carbon steel has been checked to be compatible with FERT-1 at the expected operating temperatures below 235 °C. The molten salt tank, operating between 150 and 235 °C, will be connected to different technologies of concentrating solar collectors to operate a district heating and cooling demand allowing the implementation of double-effect absorption chillers. The total volume for a capacity of 2 MWh, corresponding to 4.82 h of the solar nominal concentrated energy production, is 30,53 m^3, with 20,76 m^3 of quartzite rock.

The availability of stored heat above 150 °C increases the possibility of applying concentrated solar technologies to cover district energy demand linked to advanced absorption chillers, or even additional medium temperature (150–235 °C) thermal services. This could be an important contribution for the decarbonization of the energy consumption in the residential sector. Up to date, only biomass boilers are the renewable thermal technology that would be applied to such temperature level. The development of a thermal storage system operating between 150 and 235 °C would open the path for a complete delivery of primary energy based on solar thermal technologies to district heating and cooling. Such storage is not available at present day. The operation of a facility, as the one proposed here, to validate the application of a low-melting temperature salt mixture is a step forward for the decarbonization of the residential sector.

Table 2
Statistical comparison between the dynamic model and reported data.

	Bayón et al. [17]	Solar One [35]
Root mean square error (RMSE)	x = 12 cm; $\sqrt{(T - T_{data})^2}$=0.72 °C x = 40 cm; RMSE = 0,83 °C x = 67 cm; RMSE = 1,08 x = 95 cm; RMSE = 0.84 x = 122 cc; RMSE = 1,13	t = 0 h; RMSE = 0.22 °C t = 4 h; RMSE = 2.33 °C t = 8 h; RMSE = 5.37 °C
Maximum Temperature difference, $\frac{T - T_{data}}{\Delta T_{tank}}$ (%)	x = 12 cm; DT_{max} = 5,9 % x = 40 cm; DT_{max} = 6,2 % x = 67 cm; DT_{max} = 8,5 % x = 95 cm; DT_{max} = 5,4 % x = 122 cc; DT_{max} = 7,5 %	t = 0 h; DT_{max} = 0.71 % t = 4 h; DT_{max} = 5.1 % t = 8 h; DT_{max} = 17.7 %
Mean Temperature difference, $\frac{T - T_{data}}{\Delta T_{tank}}$ (%)	x = 12 cm; DT_m = 2,1 % x = 40 cm; DT_m = 2,4 % x = 67 cm; DT_m = 2,8 % x = 95 cm; DT_m = 2,5 % x = 122 cc; DT_m = 2,9 %	t = 0 h; DT_m = 0.15 % t = 4 h; DT_m = 2.11 % t = 8 h; DT_m = 5.07 %

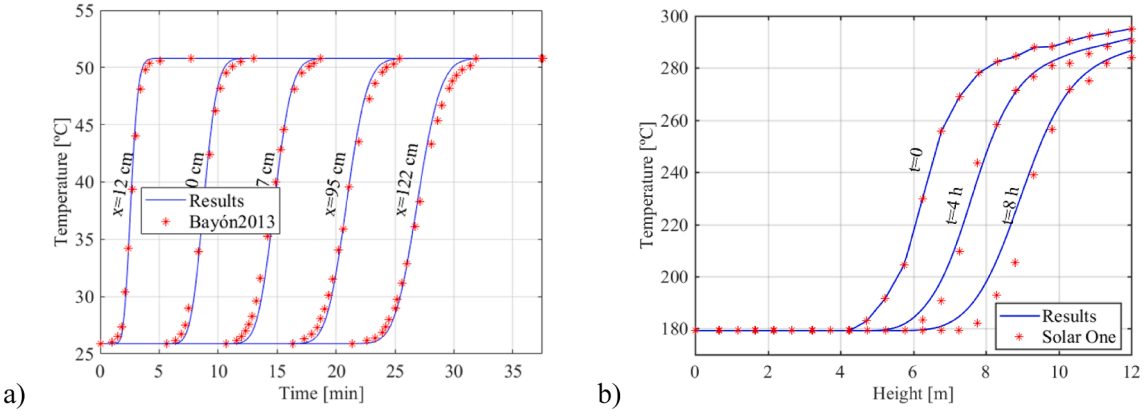

Fig. 11. Qualification of the dynamic model for a water thermocline tank (a), and a molten salt tank (b).

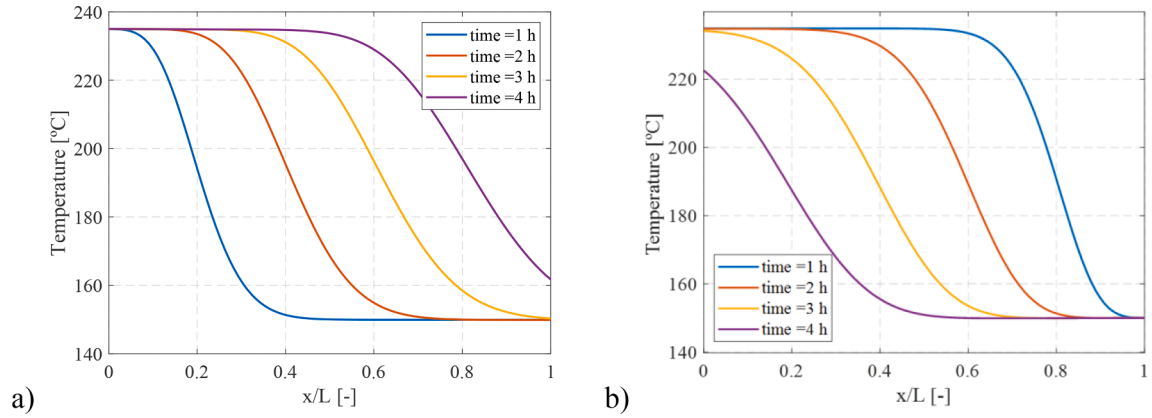

Fig. 12. Results of the charge (a) and discharge (b) thermocline evolution in the WEDISTRICT storage.

Declaration of Competing Interest

The authors declare that they have no known competing financial interests or personal relationships that could have appeared to influence the work reported in this paper.

Data availability

Data will be made available on request.

Acknowledgments

The work on this communication has been generated in the framework of the WEDISTRICT project, received funding from the European Union's Horizon 2020 research and innovation program under grant agreement N°857801.

References

[1] "WEDISTRICT," 2022. [Online]. Available: https://www.wedistrict.eu/.
[2] M. Economidou, V. Todeschi, P. Bertoldi, D. D'Agostino, P. Zangheri, L. Castellazzi, Review of 50 years of EU energy efficiency policies for buildings, Energy Build. 225 (2020) 110322, https://doi.org/10.1016/j.enbuild.2020.110322.
[3] Eurostat, "Eurostat database on Energy," 2021. [Online]. Available: http://ec.europa.eu/eurostat/web/energy/data/database.
[4] B.K. Sovacool, L.F. Cabeza, A.L. Pisello, A.F. Colladon, H.M. Larijani, B. Dawoud, M. Martiskainen, Decarbonizing household heating: Reviewing demographics, geography and low-carbon practices and preferences in five European countries, Renew. Sustain. Energy Rev. 139 (2021) 110703, https://doi.org/10.1016/j.rser.2020.110703.
[5] F. Comino, F. Táboas, F. Peci, M. Ruiz de Adana, Detailed experimental analysis of the energy performance of a desiccant wheel activated at low temperature, Appl. Therm. Eng. 178 (2020) 115580, https://doi.org/10.1016/j.applthermaleng.2020.115580.
[6] C. Prieto, R. Osuna, A.I. Fernández, L.F. Cabeza, Thermal storage in a MW scale. Molten salt solar thermal pilot facility: Plant description and commissioning experiences, Renew. Energy 99 (2016) 852–866, https://doi.org/10.1016/j.renene.2016.07.053.
[7] S.M. Flueckiger, Z. Yang, S.V. Garimella, Review of Molten-Salt Thermocline Tank Modeling for Solar Thermal Energy Storage, Heat Transf. Eng. 34 (10) (2013) 787–800, https://doi.org/10.1080/01457632.2012.746152.
[8] A.M. Bonanos, M.C. Georgiou, K.G. Stokos, C.N. Papanicolas, Engineering aspects and thermal performance of molten salt transfer lines in solar power applications, Appl. Therm. Eng. 154 (2019) 294–301, https://doi.org/10.1016/j.applthermaleng.2019.03.091.
[9] S. Frangini, A. Masi, Molten carbonates for advanced and sustainable energy applications: Part I. Revisiting molten carbonate properties from a sustainable viewpoint, Int. J. Hydrogen Energy 41 (41) (2016) 18739–18746, https://doi.org/10.1016/j.ijhydene.2015.12.073.
[10] S. Trevisan, W. Wang, R. Guedez, B. Laumert, Experimental evaluation of an innovative radial-flow high-temperature packed bed thermal energy storage, Appl. Energy 311 (2022) 118672, https://doi.org/10.1016/j.apenergy.2022.118672.
[11] J.-F. Hoffmann, T. Fasquelle, V. Goetz, X. Py, A thermocline thermal energy storage system with filler materials for concentrated solar power plants: Experimental data and numerical model sensitivity to different experimental tank scales, Appl. Therm. Eng. 100 (2016) 753–761, https://doi.org/10.1016/j.applthermaleng.2016.01.110.
[12] X. Ju, C. Xu, G. Wei, X. Du, Y. Yang, A novel hybrid storage system integrating a packed-bed thermocline tank and a two-tank storage system for concentrating solar power (CSP) plants, Appl. Therm. Eng. 92 (2016) 24–31, https://doi.org/10.1016/j.applthermaleng.2015.09.083.
[13] M. Delgado, A. Lázaro, J. Mazo, B. Zalba, Review on phase change material emulsions and microencapsulated phase change material slurries: Materials, heat transfer studies and applications, Renew. Sustain. Energy Rev. 16 (1) (2012) 253–273, https://doi.org/10.1016/j.rser.2011.07.152.
[14] H. Nazir, M. Batool, F.J. Bolivar Osorio, M. Isaza-Ruiz, X. Xu, K. Vignarooban, P. Phelan, Inamuddin, A.M. Kannan, Recent developments in phase change materials for energy storage applications: A review, Int. J. Heat Mass Transf. 129 (2019) 491–523, https://doi.org/10.1016/j.ijheatmasstransfer.2018.09.126.
[15] T. Esence, A. Bruch, J.F. Fourmigué, B. Stutz, A versatile one-dimensional numerical model for packed-bed heat storage systems, Renew. Energy 133 (Apr. 2019) 190–204, https://doi.org/10.1016/j.renene.2018.10.012.
[16] J. Raccanello, S. Rech, A. Lazzaretto, Simplified dynamic modeling of single-tank thermal energy storage systems, Energy 182 (Sep. 2019) 1154–1172, https://doi.org/10.1016/j.energy.2019.06.088.
[17] R. Bayón, E. Rojas, Simulation of thermocline storage for solar thermal power plants: From dimensionless results to prototypes and real-size tanks, Int. J. Heat Mass Transf. 60 (2013) 713–721, https://doi.org/10.1016/j.ijheatmasstransfer.2013.01.047.
[18] Y.P. Chandra, T. Matuska, Stratification analysis of domestic hot water storage tanks: A comprehensive review, Energy Build. 187 (2019) 110–131, https://doi.org/10.1016/j.enbuild.2019.01.052.
[19] F.G.F. Qin, X. Yang, Z. Ding, Y. Zuo, Y. Shao, R. Jiang, X. Yang, Thermocline stability criterions in single-tanks of molten salt thermal energy storage, Appl. Energy 97 (2012) 816–821, https://doi.org/10.1016/j.apenergy.2012.02.048.
[20] Y.A. Chang, S. Chen, F. Zhang, X. Yan, F. Xie, R. Schmid-Fetzer, W.A. Oates, Phase diagram calculation: past, present and future, Prog. Mater. Sci. 49 (3-4) (2004) 313–345, https://doi.org/10.1016/S0079-6425(03)00025-2.
[21] P. Zhang, J. Cheng, Y. Jin, X. An, Evaluation of thermal physical properties of molten nitrate salts with low melting temperature, Sol. Energy Mater. Sol. Cells 176 (2018) 36–41, https://doi.org/10.1016/j.solmat.2017.11.011.
[22] C. Villada, F. Jaramillo, J.G. Castaño, F. Echeverría, F. Bolívar, Design and development of nitrate-nitrite based molten salts for concentrating solar power applications, Sol. Energy 188 (2019) 291–299, https://doi.org/10.1016/j.solener.2019.06.010.
[23] M. Bernagozzi, A.S. Panesar, R. Morgan, Molten salt selection methodology for medium temperature liquid air energy storage application, Appl. Energy 248 (2019) 500–511, https://doi.org/10.1016/j.apenergy.2019.04.136.
[24] M.P.P.F. Galindo, F. Lorman, L. Contreras, "Composición de sales de nitrato para su uso como fluido de almacenamiento y transferencia de calor de bajo punto de fusión alta temperatura de descomposición," ES2424823, 2012.
[25] J.E. Pacheco, et al., Results of molten salt panel and component experiments for solar central receivers: Cold fill, freeze/thaw, thermal cycling and shock, and instrumentation tests, United States, 1995.
[26] D.F. Williams, Assessment of Candidate Molten Salt Coolants for the NGNP/NHI Heat-Transfer Loop. United States Department of Energy, ORNL/TM-2006/69, 2006.
[27] A.G. Fernández, M.I. Lasanta, F.J. Pérez, Molten Salt Corrosion of Stainless Steels and Low-Cr Steel in CSP Plants, Oxid. Met. 78 (5) (2012) 329–348, https://doi.org/10.1007/s11085-012-9310-x.
[28] R.W. Bradshaw, D.E. Meeker, High-temperature stability of ternary nitrate molten salts for solar thermal energy systems, Sol. Energy Mater. 21 (1) (1990) 51–60, https://doi.org/10.1016/0165-1633(90)90042-Y.
[29] V.M.B. Nunes, C.S. Queirós, M.J.V. Lourenço, F.J.V. Santos, C.A. Nieto de Castro, Molten salts as engineering fluids – A review, Appl. Energy 183 (2016) 603–611.
[30] Y. Filali Baba, H. Ajdad, A.A.L. Mers, Y. Grosu, A. Faik, Multilevel comparison between magnetite and quartzite as thermocline energy storage materials, Appl. Therm. Eng. 149 (2019) 1142–1153, https://doi.org/10.1016/j.applthermaleng.2018.12.002.

[31] J.E. Pacheco, S.K. Showalter, W.J. Kolb, Development of a Molten-Salt Thermocline Thermal Storage System for Parabolic Trough Plants, J. Sol. Energy Eng. 124 (2) (Apr. 2002) 153–159, https://doi.org/10.1115/1.1464123.
[32] S.A. Klein, "EES – Engineering Equation Solver, Version 10.836." 2021.
[33] I. MathWorks, MATLAB : the language of technical computing : computation, visualization, programming : installation guide for UNIX version 5. Natwick : Math Works Inc., 1996., 1996.
[34] T.E.W. Schumann, Heat transfer: A liquid flowing through a porous prism, J. Franklin Inst. 208 (3) (1929) 405–416, https://doi.org/10.1016/S0016-0032(29)91186-8.
[35] S.M. Flueckiger, B.D. Iverson, S.V. Garimella, J.E. Pacheco, System-level simulation of a solar power tower plant with thermocline thermal energy storage, Appl. Energy 113 (Jan. 2014) 86–96, https://doi.org/10.1016/j.apenergy.2013.07.004.